

MASS-YIELD DISTRIBUTION FOR THE PHOTOSPALLATION OF
MEDIUM-WEIGHT ELEMENTS AT INTERMEDIATE ENERGIES

M.L. Terranova, P. de Chiara and V. di Napoli
Istituto di Chimica Generale e Inorganica dell'Università
00185 Roma, Italia

J.B. Martins and O.A.P. Tavares
Centro Brasileiro de Pesquisas Físicas-CNPq
22290 Rio de Janeiro, Brasil

ABSTRACT

A semiempirical five-parameter formula is proposed, which reproduces quite satisfactorily the measured mean cross sections per photon for spallation residuals arising from target masses ranging between 27 and 118, at energies from 0.1 GeV up to 1 GeV.

Some attempts to describe the general trend of photo-spallation yields by means of multiparameter semiempirical formulae have heretofore been made (¹⁻³) with rather encouraging results, even if the measured cross sections are often reproduced with an agreement not very satisfactory (in a number of cases, a factor more than three).

A previous paper (³) presented a simple five-parameter mass-yield formula, which adequately estimated (to within a factor

of about 2) photospallation cross sections for medium-weight elements ($40 \lesssim A \lesssim 60$) at intermediate energies. Aiming to extend the validity of this formula to a wider range of target masses, we analysed a total of 176 available measured mean cross sections per photon, $\bar{\sigma}_K$, in the energy range (0.1 - 1) GeV, for target elements from $^{23}_{11}\text{Na}$ to $^{127}_{53}\text{I}$ (⁴⁻¹⁵). The analysis was carried out with the same procedure already reported in (³).

By introducing the slope K of the yield-surface ridge of isotopic distributions as a multiplying factor (³), the quantities $\sigma^* = \bar{\sigma}_K \times K^{\Delta Z}$ have been calculated (Z represents here the difference $Z_t - Z_p$ between the charge numbers of the target and product nuclei), and a least-squares analysis has been undertaken on $n = 165$ cross section data (11 points were rejected a priori for reasons which will be clear later), with a σ^* distribution (³) fitted by

$$\sigma^* = a \bar{\sigma}_N \exp \{- b(A_p - A_{mp})^2\} \quad , \quad (1)$$

which may also be written as

$$\bar{\sigma}_K = (a \bar{\sigma}_N / K^{\Delta Z}) \exp\{- b(A_p - A_{mp})^2\} \quad , \quad (2)$$

where $\bar{\sigma}_N$ stands for the mean total cross section of the interaction of a photon with a free nucleon and assumes a value of 260 μb within the energy range considered, A_p is the mass number of the spallation residual, and A_{mp} the most probable mass number for a given Z_p isotopic distribution. The quantities a, K, b, and A_{mp} represent the "free" parameters (as will be shown, A_{mp} contains two free parameters).

The best-fit values resulting from a multiple linear regression were

$$\begin{cases} a = 3.30 \pm 0.08 \\ b = 0.243 \pm 0.005 \end{cases} \quad (3)$$

For the parameter K , it is to be noted that in our previous paper (³), the much more limited range of target masses considered prevented us from deducing a relationship between such slopes and mass number A_t (a constant value $K = 1.32$ being then proposed for $51 \leq A_t \leq 59$). The more refined treatment carried out on 17 target nuclei led to the following dependence on the target mass number only, for the slope K

$$K = (1.66 \pm 0.03) \hat{A}_t^{-(0.058 \pm 0.001)} \quad , \quad (4)$$

with \hat{A}_t standing for the mass number of the target element averaged over the natural isotopic abundance.

As far as the parameter A_{mp} is concerned, a Z_p -dependence has been achieved as

$$A_{mp} = (2.28 \pm 0.07) Z_p - (2.18 \pm 0.09) \quad . \quad (5)$$

Some deduced A_{mp} values are reported in Table I, which also shows the A_s values related to the nuclear charge of the most stable isobar, as reported in ref. (¹⁶). Apart from somewhat larger discrepancies met from $Z_p \geq 40$ on, it can be noted that A_{mp} and A_s are almost the same, within the range of errors in eq. (5). On the other hand, it should be considered that A_{mp} , i.e. the mass number corresponding to the maximum of each isotopic

distribution, has a meaning quite different from that of A_S , which is related to the shape of the β -stability valley.

A correlation coefficient $|r| = 0.94$ and a reproducibility $R = 1.52$ have been obtained from the statistical treatment of the data.

In Fig. 1, σ^* values are plotted as a function of $(A_p - A_S)$. Also reported in this figure is the best-fit parabola obtained from eq. (1) by inserting the values of the parameters given by (3-5). The dashed and dot-dashed parabolas have been drawn by taking into consideration the quantities R and R^3 , respectively.

Both the values of r and R clearly indicate that the analysed data are well reproduced by eq. (2).

Let us now explain in some detail the criteria we adopted in rejecting a few points in our analysis of the experimental data available. The cross sections of photoproduction of ^{119}Te , ^{121}Te , ^{116}Sb , and ^{12}Sb from ^{127}I (5), and of ^{113}In from Sn (9) showed at a first glance extremely large deviations from the pattern observed for the other spallation products (3). Moreover, these data seemed to be somewhat conflicting with each other (for instance, the yield of ^{116}Sb is a factor about 5 larger than that of ^{120}Sb for the same target nucleus ^{127}I , and one should also consider that for $Z_p = 51$ an $A_S \approx 119$ is obtained). All these scattered points (filled circles) lie on the right-hand side of Fig. 1 and above the upper dot-dashed parabola. We wish to point out, however, that eq. (5) does not satisfactorily fit the trend of A_S for charge numbers higher than 40, and this could probably explain such anomalies.

As regards the points (filled circles in Fig. 1) which

lie below the lower dot-dashed parabola, we found too small values of the photoproduction cross sections, inconsistent with the distribution of those obtained for the same produced nuclides. These points, though, represent the yields of ^{27}Mg from ^{31}P (¹⁵), ^{28}Mg from Cl (¹¹), and ^{45}K from ^{55}Mn (¹⁴), respectively, from left to right in the figure, and a reason for such low yields may be found in the (N/Z) ratios of the product nuclei being very different from the (N/Z) of the target (¹⁷). Finally, the three points in parentheses, relative to ^{24}Na photoproduction from Sn, Ag, and Mo (from the top of Fig. 1 downward) were rejected since their formation could seriously be influenced by fragmentation processes.

Some words must be spent about the set of data obtained by Noga et al. (⁴) for the ^{24}Na photoproduction from ^{28}Si , ^{31}P , ^{32}S , $^{35.5}\text{Cl}$, ^{39}K , and ^{40}Ca . These authors found $\bar{\sigma}_K$ values considerably smaller than those measured in other laboratories. Järund et al. (⁶) showed that when multiplied by a factor of about 2, the yields of Noga et al. fitted very well the largest majority of experimental data concerning the same reactions, and suggested that such a normalising factor could be explained by the uncorrect yield monitor curve used in calculating the cross sections. Following this suggestion, we normalised in the course of the analysis the data of Noga et al. by multiplying each yield by a factor 2.

A more direct and clear comparison between experimental (σ_e) and calculated (σ_c) cross sections has been made by drawing histograms of frequency distribution of the quantity

$$\rho = (\Delta\sigma/|\Delta\sigma|) \times \{(\sigma_e/\sigma_c)^{\Delta\sigma/|\Delta\sigma|} - 1\} \quad , \quad (6)$$

with $\Delta\sigma = \sigma_e - \sigma_c$.

In Fig. 2, the frequency distribution of ρ is illustrated for the whole set of data we used in deriving eqs. (2) and (3-5). The histogram we obtained is without any doubt gaussian-shaped, and, what is still more important, centered at $\rho = 0$ and remarkably sharp. The frequency distribution of ρ for ^{24}Na photoproduction from target nuclei ranging between ^{27}Al and ^{80}Br is given in Fig. 3. Also in this case we got a distribution centred around 0, although a shift towards negative values is evident.

We wish to conclude this note by putting some emphasis in remarking as eq. (2) with the set of parameters given by (3-5) is entirely adequate in reproducing the measured yields with relatively high accuracy (within a factor 1.5 for 54% of the cases and 2.5 for more than 90% of the cases) for target elements which cover a wide region of masses (27 to 118), and this surely represents a satisfactory result.

REFERENCES

- (¹) G.J. Kumbartzky, U. Kim and C.K. Kwan: Nucl. Phys., A160, 237 (1971); G.J. Kumbartzky and U. Kim: Nucl. Phys. A176, 23 (1971).
- (²) G.G. Jonsson and K. Lindgren: Phys. Scripta, 7, 49 (1973); 15, 308 (1977).
- (³) V. di Napoli, M.L. Terranova, J.B. Martins and O.A.P. Tavares: Lett. Nuovo Cimento, 21, 83 (1978).
- (⁴) V.I. Noga, Yu. N. Ranyuk and P.V. Sorokin: Yad. Fiz., 9, 1152 (1969) (transl.: Soviet J. Nucl. Phys., 9, 673 (1969)).
- (⁵) G.G. Jonsson and B. Persson: Nucl. Phys., A153, 32 (1970).
- (⁶) A. Järund, B. Friberg and B. Forkman: Z. Physik, 262, 15 (1973).
- (⁷) V. di Napoli, G. Rosa, F. Salvetti, M.L. Terranova, H.G. de Carvalho, J.B. Martins and O.A.P. Tavares: J. Inorg. Nucl. Chem., 37, 1101 (1975).
- (⁸) M. Eriksson and G.G. Jonsson: Nucl. Phys., A242, 507 (1975).
- (⁹) B. Bülow, M. Eriksson, G.G. Jonsson and E. Hagebø: Z. Physik, A275, 261 (1975).
- (¹⁰) B. Bülow, B. Johnsson, M. Nilsson and B. Forkman: Z. Physik, A278, 89 (1976).
- (¹¹) V. di Napoli, M.L. Terranova and P. di Bernardo: Gazz. Chim. Ital., 106, 999 (1976).
- (¹²) I. Blomqvist, P. Janežek, G.G. Jonsson, R. Petersson, H. Dinter and K. Tesch: Z. Physik, A278, 83 (1976).
- (¹³) A. Järund and B. Forkman: Z. Physik, A281, 39 (1977).
- (¹⁴) V. di Napoli, F. Salvetti, M.L. Terranova, H.G. de Carvalho, J.B. Martins and O.A.P. Tavares: J. Inorg. Nucl. Chem., 40, 175 (1978).
- (¹⁵) B. Bülow, B. Johnsson and M. Nilsson: Z. Physik, A285, 323 (1978).
- (¹⁶) R.D. Evans: The Atomic Nucleus (New York, N.Y., 1969), p.292.
- (¹⁷) S. Regnier: Phys. Rev. C, 20, 1517 (1979); see also the references there quoted.

Table I - Comparison between A_{mp} and A_s for different photoproduced nuclides, as a function of Z_p (see text for further details).

Element (chemical symbol)	Z_p	A_{mp} (present work)	A_s (ref. (16))	$A_s - A_{mp}$
F	9	18.3	18.8	+ 0.5
Ne	10	20.6	21.0	+ 0.4
Na	11	22.9	23.1	+ 0.2
Mg	12	25.2	25.3	+ 0.1
Al	13	27.4	27.5	+ 0.1
Cl	17	36.6	36.4	- 0.2
Ar	18	38.9	38.6	- 0.3
K	19	41.1	40.9	- 0.2
Ca	20	43.4	43.1	- 0.3
Sc	21	45.7	45.4	- 0.3
V	23	50.3	50.1	- 0.2
Cr	24	52.5	52.4	- 0.1
Mn	25	54.8	54.7	- 0.1
Fe	26	57.1	57.1	0
Co	27	59.4	59.4	0
Ni	28	61.7	61.8	+ 0.1
Cu	29	63.9	64.2	+ 0.3
As	33	73.1	73.7	+ 0.6
In	49	109.5	114.1	+ 4.6
Sb	51	114.1	119.3	+ 5.2
Te	52	116.4	122.0	+ 5.6
I	53	118.7	124.6	+ 5.9

FIGURE CAPTIONS

Fig. 1 - Trend of $\sigma^* = \bar{\sigma}_K \times K^{\Delta Z}$ as a function of $(A_p - A_{mp})$. The upper and lower dot-dashed parabolas (i.e. $\sigma^* \times R^{\pm 3}$) determine the area which contains more than 99% of the points (open circles) considered in the analysis. The filled circles and the circles between parentheses refer to data rejected a priori. For further details, see text.

Fig. 2 - Frequency distribution of ρ (as defined by eq. (6) of the text) for $n = 165$ experimentally determined cross sections (these are the same indicated with open circles in Fig. 1).

Fig. 3 - Frequency distribution of ρ for ^{24}Na photoproduction from different target nuclei ($n = 34$).

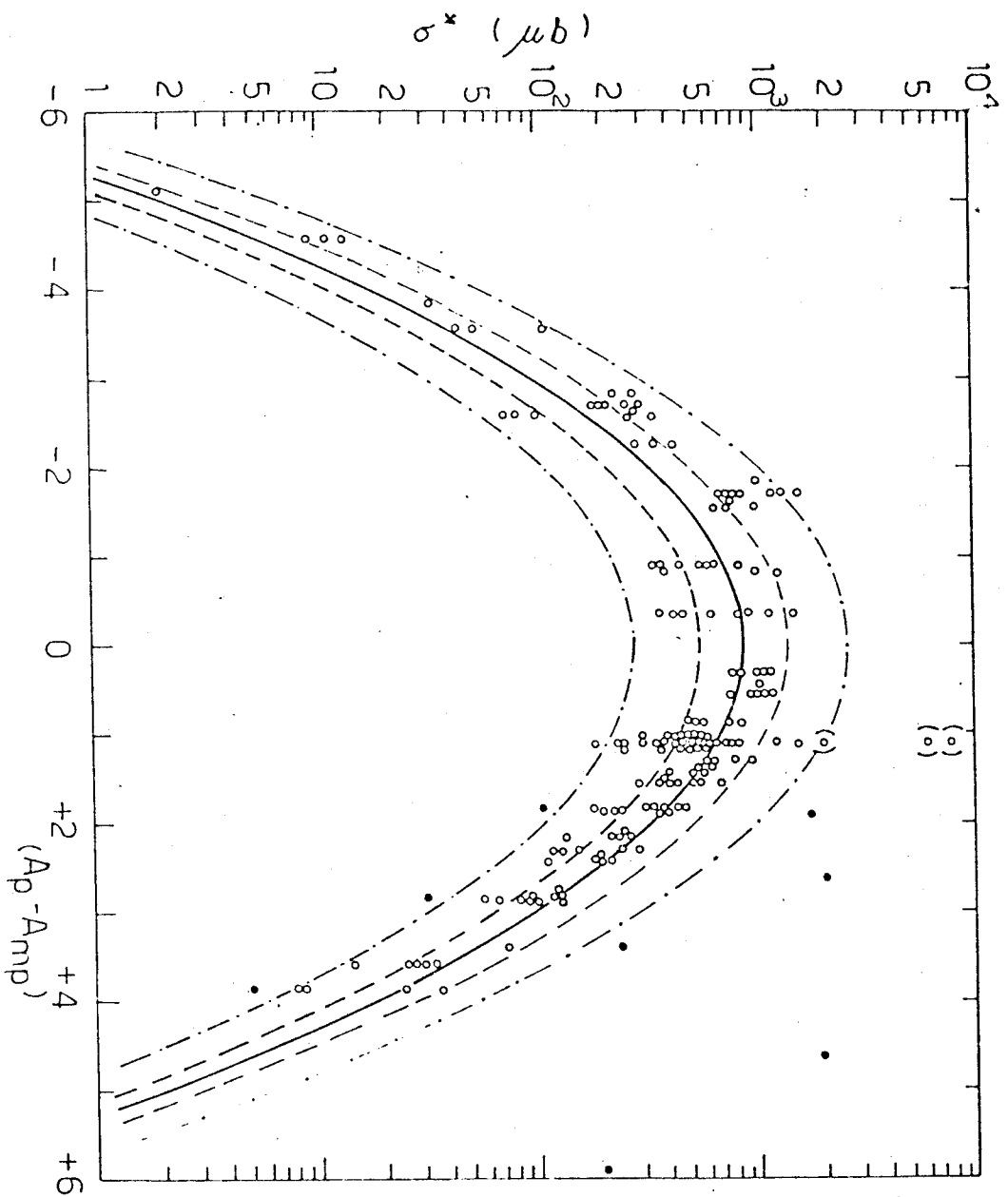


Figure 1

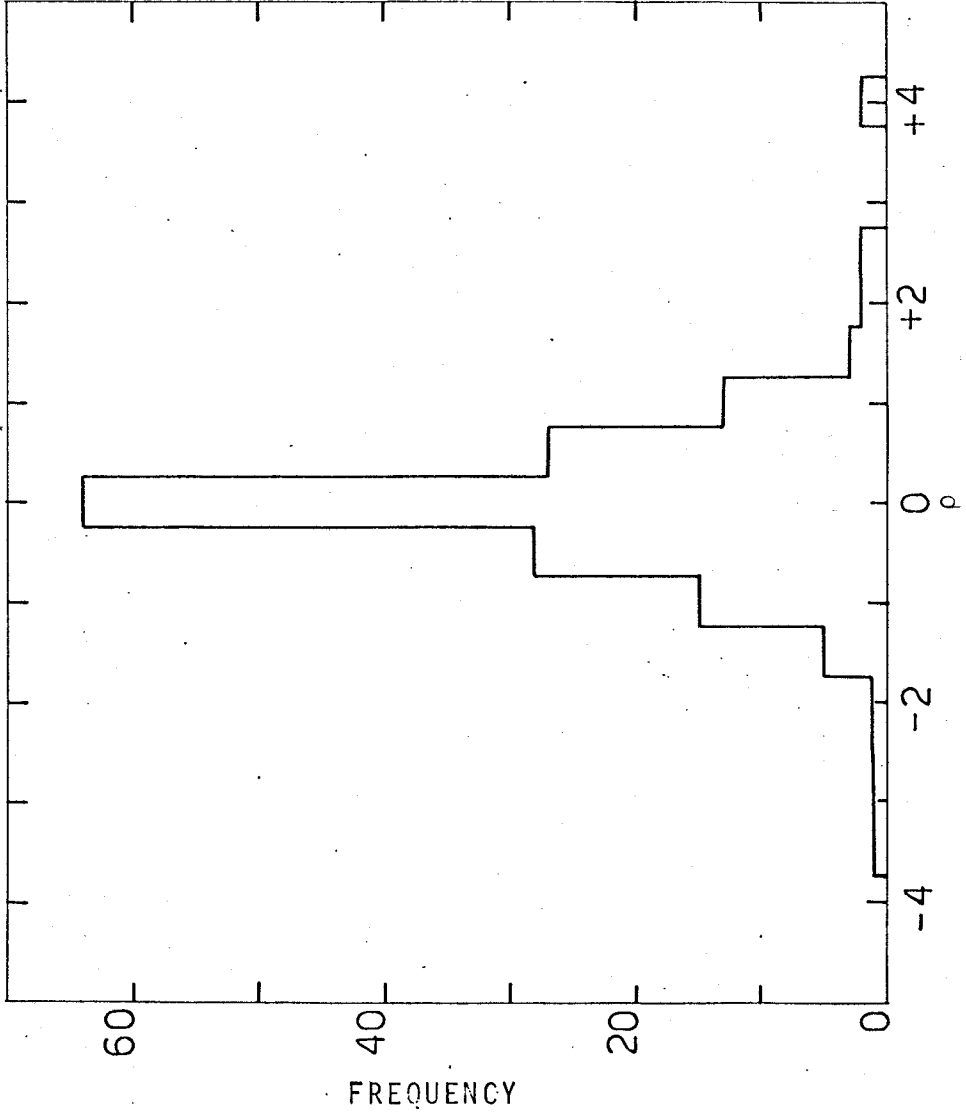


Figure 2

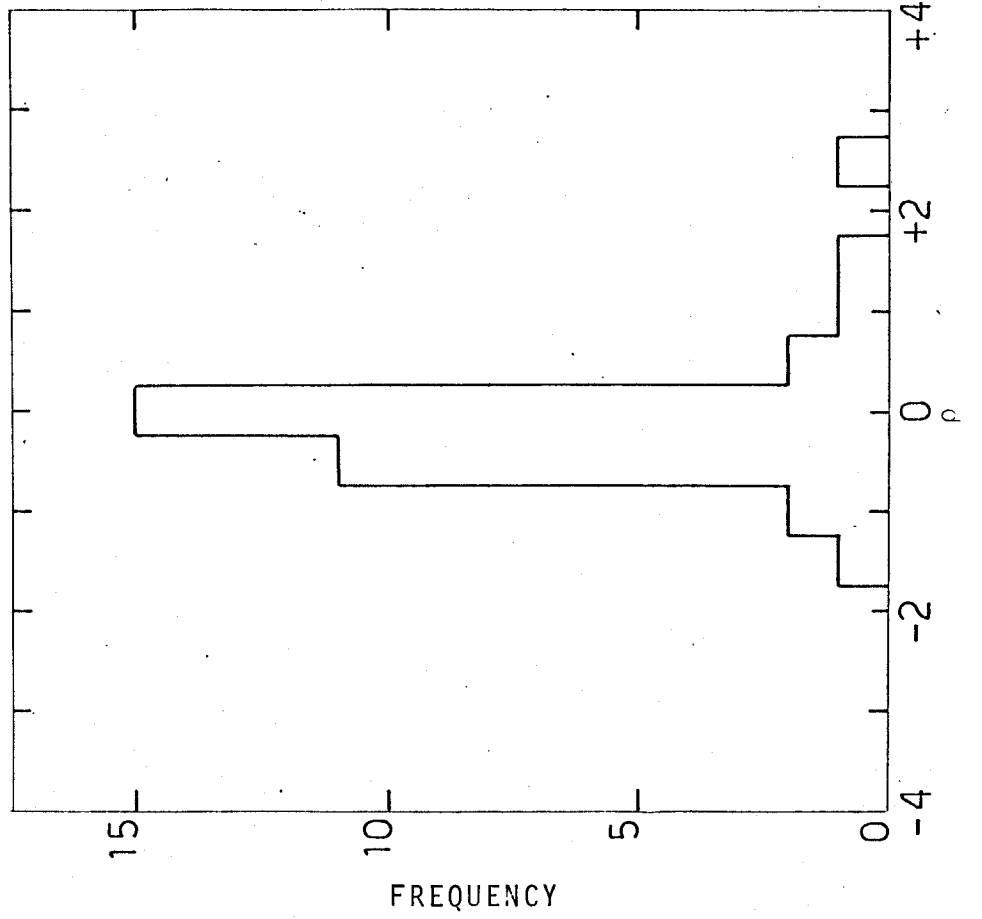


Figure 3